



Review

Review of Hydrogen Storage in Solid-State Materials

Gelin Chen ^{1,2,3}, Deqing Liang ^{1,2,3,*}, Zhanxiao Kang ⁴, Jintu Fan ⁴, Shuanshi Fan ⁵ and Xuebing Zhou ^{1,2,3,*}

- Guangzhou Institute of Energy Conversion, Chinese Academy of Sciences, Guangzhou 510640, China; chengelin@mail.ustc.edu.cn
- School of Energy Science and Engineering, University of Science and Technology of China, Hefei 230026, China
- Guangdong Provincial Key Laboratory of New and Renewable Energy Research and Development, Guangzhou 510640, China
- School of Fashion and Textiles, The Hong Kong Polytechnic University, Hong Kong, China; z.x.kang@polyu.edu.hk (Z.K.); jin-tu.fan@polyu.edu.hk (J.F.)
- School of Chemistry and Chemical Engineering, South China University of Technology, Guangzhou 510641, China; ssfan@scut.edu.cn
- * Correspondence: liangdq@ms.giec.ac.cn (D.L.); zhouxb@ms.giec.ac.cn (X.Z.); Tel./Fax: +86-20-8705-7653 (X.Z.)

Abstract: As a kind of clean energy, hydrogen energy has great potential to reduce environmental pollution and provide efficient energy conversion, and the key to its efficient utilization is to develop safe, economical and portable hydrogen storage technology. At present, hydrogen storage technology lags behind hydrogen production and use, which is the bottleneck restricting the development of hydrogen energy. In this paper, several current solid-state hydrogen storage methods are reviewed, including hydrate hydrogen storage, alloy hydrogen storage and MOF hydrogen storage. At the hydrogen storage density level, the hydrogen storage capacity of 1K-MOF-5 can reach 4.23 wt% at 77 K and 10 MPa, and remains basically unchanged in 20 isothermal adsorption and desorption experiments. At the level of temperature and pressure of hydrogen storage, the alloy can realize hydrogen storage under ambient conditions. At the economic level, the cost of hydrogen storage in hydrates is only USD 5-8 per kilogram, with almost zero carbon emissions. Through the analysis, it can be seen that the above solid-state hydrogen storage technologies have their own advantages. Although hydrate hydrogen storage is lower than alloy materials and MOF materials in hydrogen storage density, it still has huge potential for utilization space because of its low cost and simple preparation methods. This paper further provides a comprehensive review of the existing challenges in hydrate research and outlines prospective directions for the advancement of hydrogen storage technologies.

Keywords: hydrogen storage; MOFs; alloy; hydrate; clean energy



Academic Editors: Vincenzo Liso and Samuel Simon Araya

Received: 20 March 2025 Revised: 25 May 2025 Accepted: 27 May 2025 Published: 3 June 2025

Citation: Chen, G.; Liang, D.; Kang, Z.; Fan, J.; Fan, S.; Zhou, X. Review of Hydrogen Storage in Solid-State Materials. *Energies* **2025**, *18*, 2930. https://doi.org/10.3390/en18112930

Copyright: © 2025 by the authors. Licensee MDPI, Basel, Switzerland. This article is an open access article distributed under the terms and conditions of the Creative Commons Attribution (CC BY) license (https://creativecommons.org/licenses/by/4.0/).

1. Introduction

Human energy utilization has been developing in the direction of low carbon. In the 21st century, the mode of resource development and utilization has changed from mineral resource consumption to natural resource regeneration, and the development and utilization of hydrocarbon fuel has changed from high-carbon fuel to low-carbon fuel [1,2]. Hydrogen energy has been widely valued for its advantages such as high calorific value, non-pollution and renewable. Over the past decade, China's hydrogen energy industry has achieved significant growth [3]. In 2015, China's hydrogen production was approximately 20 million tons, and by 2023, the national hydrogen production exceeded 35 million tons, with an average annual growth rate of about 2.3% [4–6]. Meanwhile, the utilization of

Energies **2025**, 18, 2930 2 of 22

hydrogen energy has also increased substantially. In 2021, the market size of the global hydrogen energy industry reached USD 155 billion, and it was expected to surpass USD 250 billion by 2025, with an average annual growth rate of over 12–18% [7]. It is a promising secondary energy in the 21st century and an important direction of the global energy technology revolution. Many countries are stepping up the deployment of hydrogen energy strategies. The hydrogen economy, which focuses on the preparation, storage, transportation and transformation of hydrogen energy, has become an ideal economic structure for the future [8–10].

The great breakthrough in hydrogen production technology has opened up a broader prospect for the wide utilization of hydrogen energy. In the field of transportation, with its advantages of zero emission and long range, hydrogen fuel cell vehicles are expected to gradually replace traditional fuel vehicles and become the mainstream choice for green travel in the future [11,12]. Hydrogen can be used as clean energy in the high energy consumption production process of iron and steel, chemical and other industries, helping traditional industries to achieve energy saving, emission reduction and green transformation [13]. In distributed power generation, hydrogen energy can provide reliable power for communities, data centers and other places stably through the combination of fuel cells and energy storage systems, and improve the security and flexibility of energy supply [14,15]. The expansion of this series of hydrogen energy utilization scenarios will greatly promote the optimization and upgrading of the global energy structure and contribute key forces to the fight against climate change and the realization of sustainable development goals [13]. However, hydrogen energy is not yet widely circulated due to limitations in transmission and storage technologies, and the vast majority of hydrogen industries are geographically close to hydrogen manufacturing plants [16]. It is difficult for hydrogen to be transported over long distances to achieve wide-scale applications. Compared with the traditional energy transportation cost, the transportation cost of hydrogen energy is the highest, as shown in Table 1 [17], transportation costs for hydrogen are still much higher than those for traditional fossil energy sources [18]. In the process of the vigorous development of hydrogen energy, the deficiency of the intermediate link of hydrogen storage has become increasingly prominent, which has become a key bottleneck restricting its further large-scale application.

Table 1. List of mode of transportation and their cost [17].

Mode of Transportation	Cost
state hydrogen trailers	1.5–3 USD/kg
liquid hydrogen tankers	2–4 USD/kg
pipeline transportation	0.5–1.5 USD/kg
pipelines	0.05–0.15 USD per liter
oil tankers	0.02–0.05 USD per liter
rail/road tankers	0.1–0.3 USD per liter
gas transportation	$0.001-0.03 \text{ USD/m}^3$

Current hydrogen storage technologies include high-pressure gaseous hydrogen storage [19,20], liquid hydrogen storage [21] and solid hydrogen storage [22]. However, high-pressure gaseous hydrogen storage (typically at 35–70 MPa) faces challenges such as high system weight (\sim 5–6 wt%), high cost (\sim 15–20 USD/kWh for Type IV tanks), and limited volumetric density (\sim 40 kg/m³ at 70 MPa). In contrast, liquid hydrogen (LH₂) storage requires cryogenic conditions (20–25 K), resulting in significant energy penalties (\sim 30–40% of hydrogen's energy content for liquefaction) and boil-off losses (\sim 0.5–1% per day) [23–25].

Energies 2025, 18, 2930 3 of 22

Both of them are difficult to realize safe, efficient, large-scale and low-cost hydrogen storage and transportation. This not only limits the wide popularity of hydrogen energy in the field of fuel cell vehicles, leads to slow progress in the layout of hydrogen filling stations due to the inconvenience of hydrogen storage and transportation, but also hinders the further expansion of hydrogen energy in distributed energy systems, industrial energy storage and other scenarios, making it difficult for the hydrogen industry chain to form a complete and smooth cycle, and the current booming solid hydrogen storage technology is expected to break this deadlock [26,27].

Solid-state hydrogen storage technology is a technology for storing hydrogen in solid materials [22]. It realizes the reversible storage of hydrogen through physical or chemical adsorption, analysis and other reactions. Solid-state hydrogen storage technology includes metal hydride hydrogen storage, carbonaceous materials that store hydrogen and metalorganic framework materials that store hydrogen [28]. Metal hydride hydrogen storage is a method of storing hydrogen by reacting metals or alloys with hydrogen to produce metal hydrides. Carbonaceous materials that store hydrogen rely on porous structures such as activated carbon to absorb hydrogen. Metal-organic frameworks (MOFs) store hydrogen, making use of their unique porous structure and adjustable hydrogen storage [29,30]. Solid-state hydrogen storage technology has the advantages of high safety, high hydrogen storage density, relatively low energy consumption and a good reversible cycle. It has a broad application prospect in transportation, energy industry and other fields, and is expected to promote the large-scale application and development of hydrogen energy [31,32].

This paper presents a comparative analysis of three major solid-state hydrogen storage technologies—metal—organic frameworks (MOFs), alloy hydrides, and hydrogen clathrate hydrates—focusing on their potential for practical hydrogen storage applications. While MOFs and metal hydrides generally demonstrate superior hydrogen storage capacities, our analysis reveals that clathrate hydrates possess distinct advantages in terms of cost-effectiveness and operational simplicity. Despite their relatively lower storage density, the economic and technical benefits of clathrate hydrates suggest significant potential for large-scale implementation. This study aims to provide valuable insights for guiding future research and development efforts in hydrogen storage technologies, particularly in identifying the most promising approaches to support the growing hydrogen economy. The findings highlight how different storage methods may be suited for specific applications, contributing to a more nuanced understanding of hydrogen storage solutions [27,33].

2. MOF Hydrogen Storage

2.1. Concept of MOF Hydrogen Storage

The concept of MOF hydrogen storage is shown in Figure 1. MOFs are a new class of porous nanomaterials bridged by metal ions or clusters with organic ligands, featuring a large specific surface area, high porosity, designable structure and easy functionalization of metal centers and ligands [34]. It has been widely used in the fields of gas adsorption separation, catalytic reaction and electrochemical energy storage. It also shows potential applications in hydrogen storage [35].

Energies 2025, 18, 2930 4 of 22

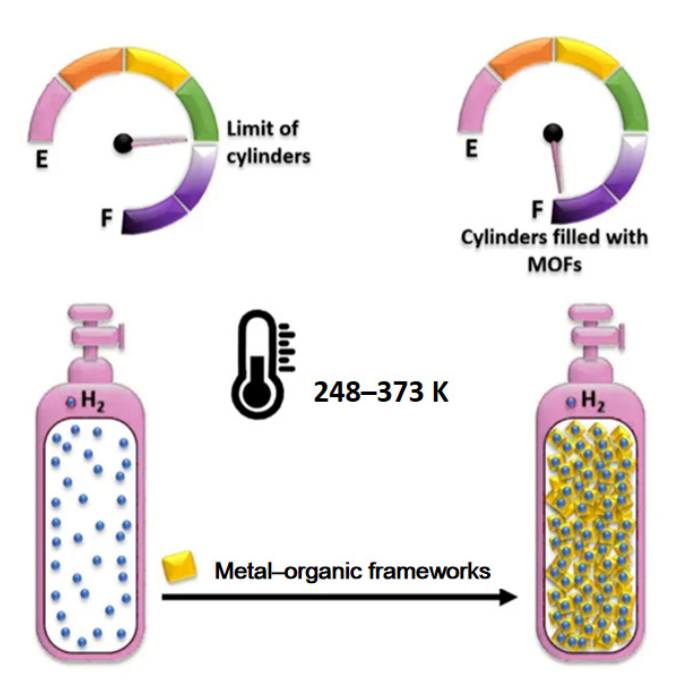


Figure 1. Schematic diagram of MOF hydrogen storage (modified from [35]).

2.2. MOF Hydrogen Storage Density

MOFs have attracted wide attention from researchers since it was first discovered in 1990 by Prof. Omar M. Yaghi [36,37]. MOF material shows great hydrogen absorption capacity at low temperatures and high pressures, which makes it an ideal material for solid-state hydrogen storage materials. However, in practical application, its low adsorption enthalpy and poor stability limit its performance, which is mainly improved by increasing specific surface area, expanding porosity, increasing active sites and changing environmental conditions [38–40]. In 2003, Yaghi et al. [41] made MOF-5 materials using Zn²⁺ salts and 4-terephthalic acid organic ligands. It was found that the hydrogen storage capacity of MOF-5 could reach 1.3 wt% at 100 kPa and 77 K. This is the first report of MOF-5 materials. After that, the experimental results show that the hydrogen storage density of MOF-5 can reach 2.49 wt% under this condition.

A report in 2017, where Deng and co-workers computationally examined a series of IRMOFs is discussed [42]. They showed in their leading example that doping IRMOF-9 with the Li+ substantially increased near-ambient hydrogen storage. IRMOF9 has a 298 K and 100 bar gravimetric uptake of just \sim 0.35 wt.% and a volumetric uptake of \sim 4.5 g/L. It was showed in Table 2. With Li+ doping, these values increase to \sim 4.5 wt.% and 27.5 g/L at 298 K and 100 bar. This corresponds to an almost 13-fold increase in gravimetric performance and a 6-fold increase in volumetric performance.

The lithiation of aromatic porous MOFs is expected to generate structures in which the lithium ion is associated with the aromatic cores. The effect of increasing the number of aromatic sites in a MOF for lithium doping was examined by Goddard and co-workers [43]. They found lithiation significantly improved hydrogen uptake at near-ambient temperatures from ~0.5 to 1.0 wt% to 2 to 5 wt%. Additionally, they found that the greater the number of aromatic cores for lithiation, the greater the hydrogen uptake. Further, they showed that lithiation directly increased binding enthalpies from the physisorption (4 to 6 kJ/mol) to chemisorption (17 kJ/mol) regimes.

Energies **2025**, *18*, 2930 5 of 22

Table 2. List	t of selected MOFs	explored with	n alkali metal	doping and	l reported H ₂	sorption at
near-ambient	temperatures [35].					

MOFs	Temperature (K)	Pressure (MPa)	Hydrogen Storage Density (wt%)	References
MOF-5	77	0.1	2.49	[44]
1Li-MOF-5	77	0.1	3.09	[44]
2Na-MOF-5	77	0.1	4.18	[44]
1K-MOF-5	77	0.1	4.23	[44]
$Cu_3(BTC)_2$	77	0.1	2.41	[45]
$LiCu_3(BTC)_2$	77	0.1	3.50	[45]
MIL-101(Cr)	77	0.1	2.37	[45]
LiMIL-101(Cr)	77	0.1	3.39	[45]
IRMOF-9	298	10	~0.35	[46]
MOF-C30	300	10	~1.0	[43]
Li-MOF-C30	300	10	~5.0	[43]

2.3. Thermodynamics Conditions of MOF Hydrogen Storage

In 2023, Farha et al. [47] reported an air-stable CuI-MOF (NU-2100). It was comprised of two distinct CuI environments, a coordinately saturated tetrahedral species and an unsaturated, almost-linear two-coordinate CuI species. The almost-linear CuI species was able to bind H_2 . The framework has an exceptionally high initial binding enthalpy of -32 kJ/mol, one of the highest reported to date [48,49]. As seen in Figure 2, this corresponds to about 1% of the CuI linear species actively binding to H_2 . At 298 K and 100 bar, NU-2100 has a volumetric capacity of 7.2 g/L H_2 .

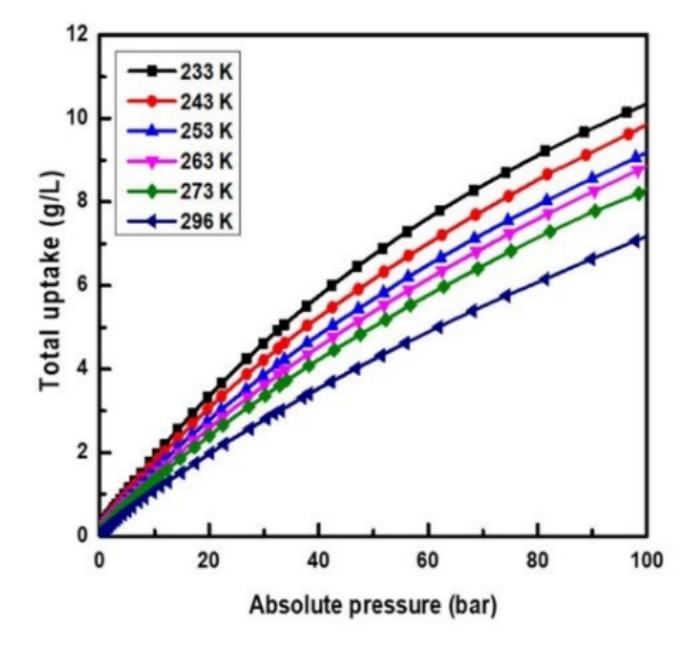


Figure 2. Adsorption isotherms (0–100 bar) of NU-2100 with hydrogen between temperatures of 296 K and 233 K.

Figure 3 indicates high-pressure near-ambient temperature isotherms for $V_2Cl_{2.8}$. It can be seen that at 208 K, the absorption rate of hydrogen is the highest. As the temperature rises, the absorption rate of hydrogen decreases accordingly. Neutron powder diffraction and spectroscopic studies revealed the H_2 was bound at the V(II) open metal sites in a Kubas-type interaction which stemmed from an interaction between the vanadium $d\pi$ and H_2 σ^* orbital [50,51]. The V-D₂ distance from neutron diffraction was the shortest metal-D₂

Energies **2025**, 18, 2930 6 of 22

bond reported in a MOF to date. This strong interaction was associated with a binding enthalpy of -21 kJ/mol, considered to be in the ideal regime for near-ambient temperature hydrogen storage [52].

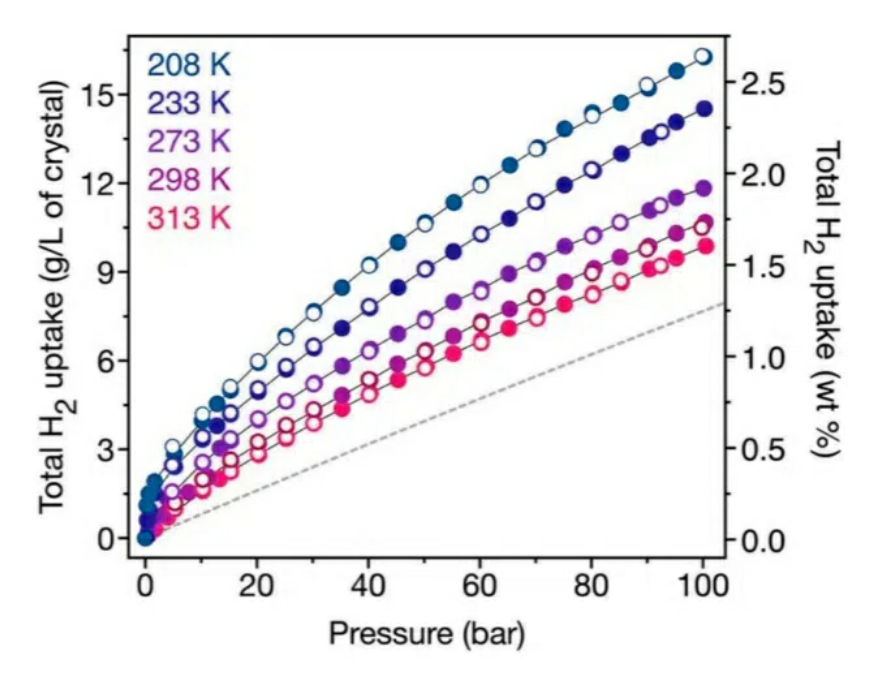


Figure 3. High-pressure near-ambient temperature isotherms for $V_2Cl_{2.8}$ (bttd). Dashed grey line indicates the volumetric density of hydrogen stored in a cylinder at 298 K (modified from [35]).

2.4. Stability of MOF Hydrogen Storage Cycle

There are perhaps two key issues to consider when discussing the stability of MOFs with respect to hydrogen storage. Firstly, MOFs must be able to cycle (from 1/4 to full), at least 1500 times, with minimum performance loss according to DOE (Department of Energy) target requirements [42]. Further, the benchmark for hydrogen purity for MOF-based adsorbents has not been set. It is likely that hydrogen storage of MOFs should withstand a range of trace impurities, including ammonia, hydrogen sulfide, hydrochloric acid, water, carbon monoxide, carbon dioxide, methane, oxygen, nitrogen and helium [53–55].

In 2019, Allendorf et al. [56] tested twelve MOFs for their stability to both static pressure (70 MPa) and cycling (5 to 100 bar, 1000 pressure cycles as depicted in Figure 4). To determine if the porosity of the framework was affected by either static or cycling hydrogen experiments, they performed a 77 K nitrogen isotherm both before and after the experiment [57]. From these results, the majority of MOFs retained their initial pore void volume, with only a small decrease of between 5 and 16% in pore volume for Mg-IRMOF-74-I and NOTT-100. The authors attributed this loss in porosity to physical damage to the MOFs, rather than chemical damage to the framework. This is thought to be the result of an abrupt pressure change during the hydrogen exposure tests. In real-world systems, this could potentially be avoided with an engineered dosing scheme for both adsorption and desorption that limits sudden pressure changes.

Energies **2025**, 18, 2930 7 of 22

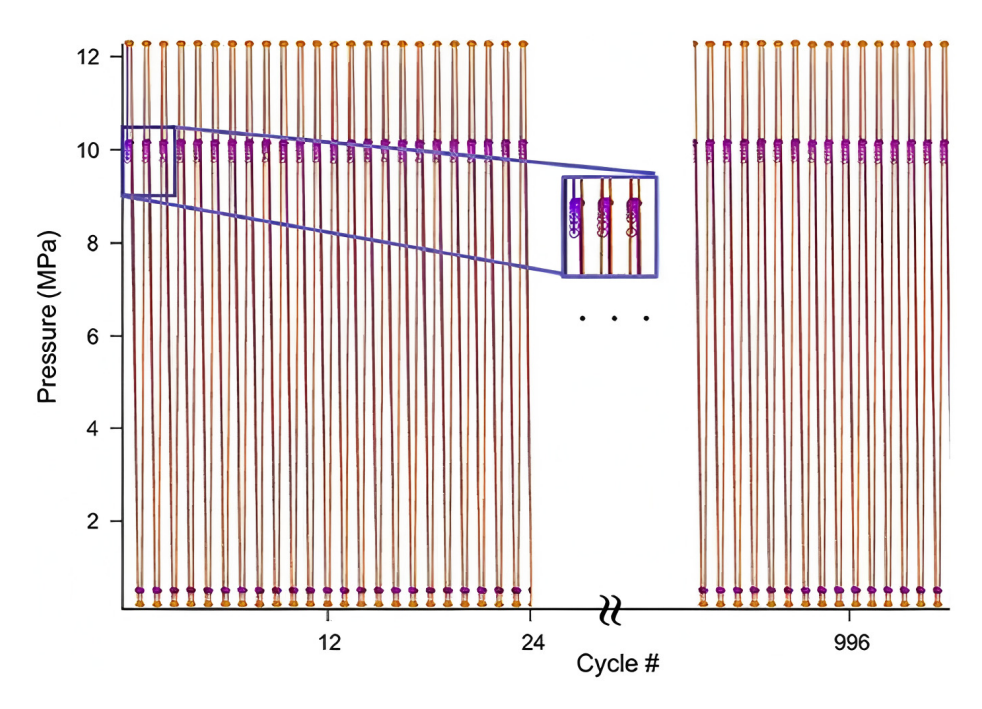


Figure 4. Hydrogen cycling experiments in the presence of MOF. Inset shows the equilibration of pressure over time (modified from [35]).

In 2016, Siegel et al. [58] undertook an extensive investigation looking at hydrogen adsorption in MOF-5 with the impact of trace impurities. These measurements were conducted at 77 K. They characterized their MOF sample before and after dosing with a hydrogen source spiked with a known quantity of impurity. The performance of MOF-5 was not impacted by most impurities, with the largest deviation (~2.5% loss) observed for 9 ppm hydrogen chloride. These results suggest that MOF-5 is relatively stable to these tested impurities in the hydrogen fuel stream [59]. It would be encouraging to see similar results replicated at near-ambient temperatures, where the impurities could be more reactive. Also worthy of more attention is whether MOFs with redox-active open metal sites are affected by trace impurities [60,61].

2.5. Commerciality of MOF Hydrogen Storage

The material cost of metal–organic frameworks (MOFs) directly affects the economic feasibility of their large-scale application. When the raw material prices rise or the preparation process becomes more complex, leading to an increase in costs, the market competitiveness of MOFs in the hydrogen storage field will significantly decline [62]. This study takes typical working conditions as an example, setting the cost of MOFs at USD 15 per kilogram as the benchmark, and comparing and analyzing two scenarios of USD 5 per kilogram and USD 25 per kilogram. Experimental data show that under the conditions of 150 bar and 210 K, most MOF systems can achieve the lowest graded hydrogen storage cost (LCOS); some materials are further optimized to the range of 170–250 K and 120–150 bar (see Figure 5b). This conclusion takes into account multiple factors such as hydrogen liquefaction energy consumption, low-temperature maintenance costs, high-pressure compression expenses, etc. [63,64].

Energies **2025**, 18, 2930 8 of 22

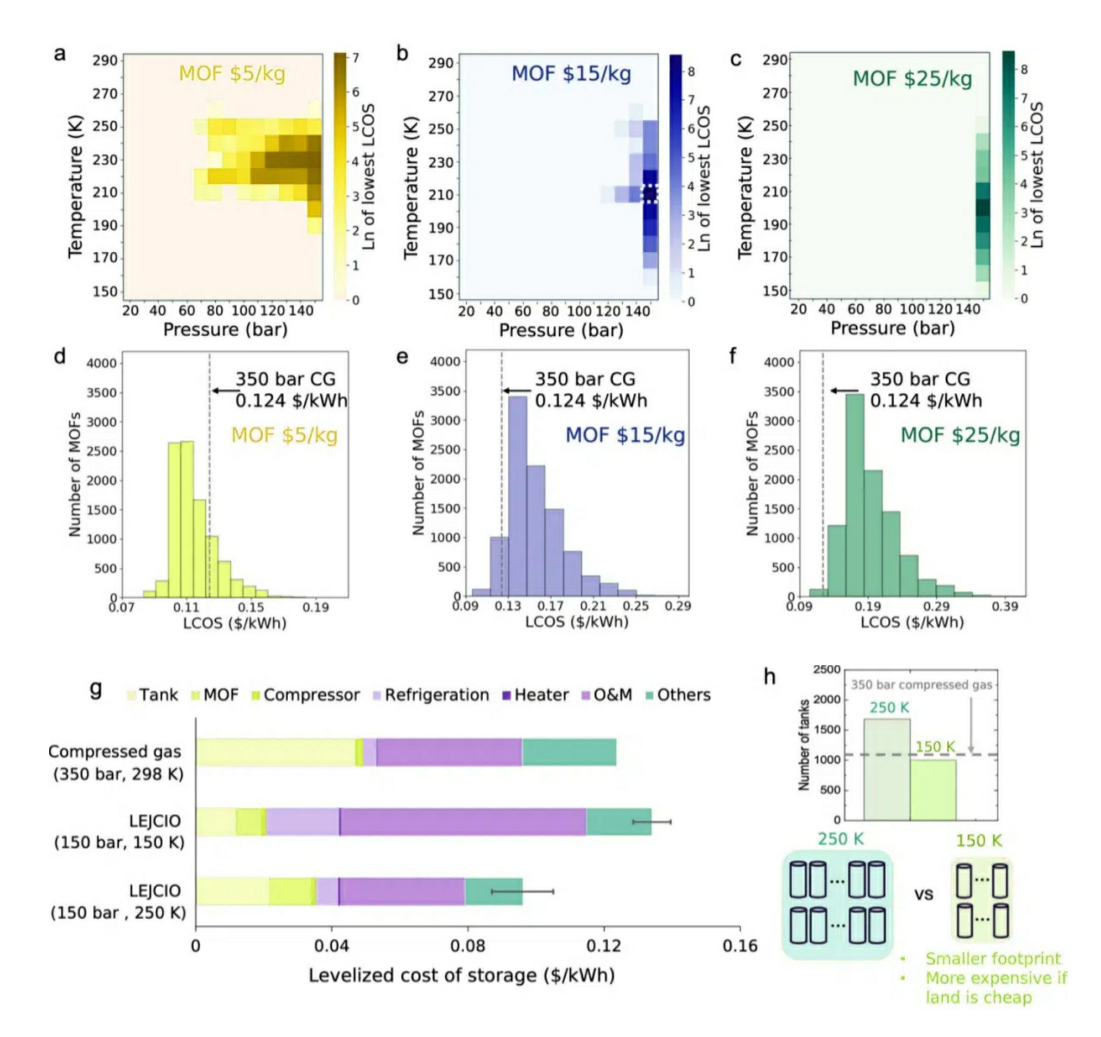


Figure 5. (**a–c**) This figure presents the optimal temperature–pressure operating windows for MOFs in backup power systems, evaluated across three cost scenarios: 5 USD/kg, 15 USD/kg and 25 USD/kg MOF pricing. (**d–f**) The corresponding probability density plots illustrate each MOf's minimum LcOs performance at its optimal conditions under these pricing regimes, with the dashed reference line indicating 350 bar compressed hydrogen's performance at 298 K. (**g**) For a representative metal–organic frame (MOF), a cost comparison analysis of it under two different operating conditions was carried out, and it was compared with the 350-bar compressed hydrogen storage method. The error line is used to quantify the impact resulting from the variation of the MOF cost within the range of 5 USD/kg to 25 USD/kg. (**h**) The required storage vessel quantities are contrasted between compressed hydrogen systems and MOF-based solutions under two operational modes, highlighting the fundamental trade-off between system footprint and associated costs at 150 K versus 250 K operating temperatures (modified from [65]).

The physical adsorption process exhibits significant temperature and pressure dependence: reducing the temperature or increasing the pressure can enhance the hydrogen storage capacity, but it will simultaneously increase the power consumption of refrigeration equipment and compressors. Different MOF materials exhibit differentiated high-pressure response characteristics due to their unique pore topological structures and distribution of active sites. It is worth noting that merely pursuing high hydrogen storage capacity will lead to increasing marginal costs, and a systematic design is needed to achieve the optimal balance between performance and cost.

When the MOF benchmark price was adjusted to USD 25 per kilogram, the lowest cost operating range shifted to 160–240 K and 150 bar (the optimal condition was 200 K and 150 bar, data source [65]). Figure 5a,c visually presents the distribution of the optimal operating parameters under different price systems.

Energies **2025**, 18, 2930 9 of 22

Figure 5d–f illustrate the transmission effect of MOF raw material costs on the system's economy: when the cost per kilogram is USD 5, the equivalent cost of the liquid carbon dioxide hydrogen storage system is USD 0.08–0.16 per kilowatt-hour; when it is USD 15, it rises to USD 0.10–0.25; and when it is USD 25, it expands to USD 0.10–0.40. It is worth noting that when the MOF price is USD 15 per kilogram, there are still 362 materials superior to 350 bar high-pressure hydrogen storage (with a compression cost of USD 0.124 per kilowatt-hour, data marked [66]), and this number drops sharply to 96 when the unit price rises to USD 25 [67,68].

3. Solid Alloy Hydrogen Storage

3.1. Concept of Hydrogen Storage in Solid Alloys

The principle of hydrogen storage in solid alloy refers to the process of hydrogen storage in solid alloy materials, which generally involves the steps of adsorption, desorption, diffusion and storage [69]. After entering the microstructure of the solid material, hydrogen will form an alloy with specific elements in the material, and then achieve storage. The understanding and research of the hydrogen storage principle of solid alloys is very important for the development of efficient and reliable hydrogen storage materials. In the principle of hydrogen storage in solid alloys, adsorption is one of the key steps, and the adsorption process can be realized by controlling the pore size and distribution of solid materials, as shown in Figure 6. The results show that the solid materials with uniform pore distribution and small pore distribution have better adsorption properties for hydrogen.

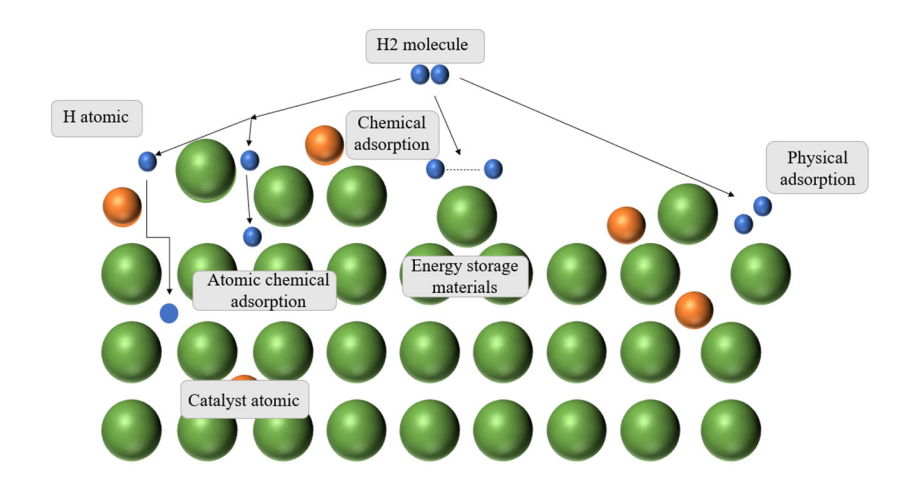


Figure 6. Mechanism of alloy hydrogen storage materials.

In a word, the principle of hydrogen storage in solid alloys realizes the high-density storage of hydrogen through the steps of adsorption, desorption, diffusion and storage. The research on the principle of hydrogen storage in solid alloys provides a theoretical basis for the development of efficient and reliable hydrogen storage materials, and makes an important contribution to promoting the application and development of hydrogen energy [70].

3.2. Hydrogen Storage Density of Alloy

High-entropy alloys, as a new type of metal hydrogen storage material, are characterized by optimizing the storage performance through the synergistic effect of multiple component elements. These materials are typically composed of various elements mixed in a nearly equal molar ratio to form a unique microstructure [71,72]. In the composite hydride system, transition metals and non-transition metals (often labeled as A-site elements) or non-metal elements (B-site elements) can form stable composite anions by chemically

Energies **2025**, 18, 2930 10 of 22

bonding hydrogen atoms. This structure often requires the involvement of alkali metal or alkaline earth metal atoms to enhance stability [73].

Solid hydrogen storage alloys can be classified into four typical systems based on their crystal structure and chemical composition, namely AB₅ type, AB₂ type, AB type and A₂B type alloys. These four types of materials exhibit different hydrogen adsorption sites and diffusion kinetics characteristics due to the differences in crystal field environments, thereby showing significantly different hydrogen storage capacity and cycling performance (Figure 7). Among them, the symmetry change of the crystal structure directly affects the hydrogen diffusion energy barrier, while the change in electronic structure plays a crucial regulatory role in hydrogen binding energy.

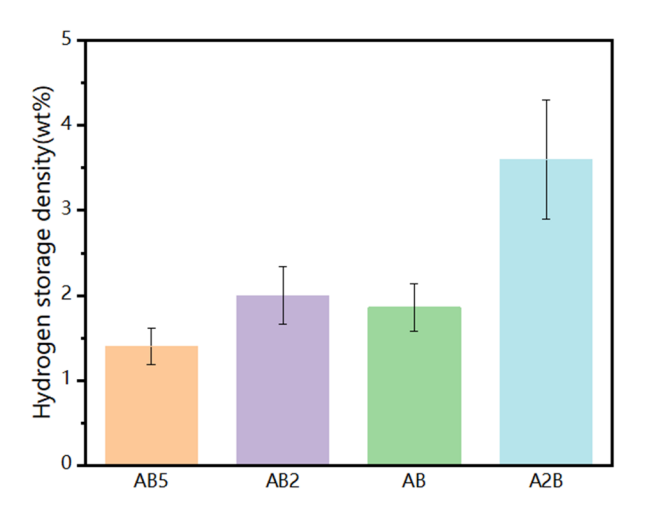


Figure 7. Hydrogen storage density of various alloys.

 AB_5 alloy is composed of rare earth metals, transition metals and hydrogen atoms, and has a high hydrogen storage capacity and a fast hydrogen absorption and desorption rate [74,75]. According to statistics, the hydrogen storage capacity of AB_5 alloy can reach 1.4 wt%, which can meet the needs of many hydrogen storage systems. AB_2 alloy is mainly composed of transition metals and hydrogen atoms. It was showed in Table 3, compared with AB_5 alloy, the hydrogen storage capacity of AB_2 alloy is slightly lower, usually 2.0 wt% [76]. However, AB_2 alloy has better cycle stability and lower preparation cost, so it has been widely used in some commercial applications. AB-type alloy is composed of two different metals and has good cycle stability. Their hydrogen storage capacity is usually 1.86 wt%, and the hydrogen absorption and desorption rate are fast. A_2B alloy is a kind of solid alloy hydrogen storage material characterized by a face-centered cubic structure [77]. It has high hydrogen storage capacity and fast hydrogen adsorption and desorption rate, so it is one of the hotspots in the research. The hydrogen storage capacity of A_2B alloy can reach 3.6 wt%, which is one of the highest among hydrogen storage materials at present.

Table 3.	Classifica	tion of l	nydrogen	i storage a	lloys	[78].	
----------	------------	-----------	----------	-------------	-------	-------	--

Hydrogen Storage Alloy	Represents Alloy	Temperature (K)	Quality Hydrogen Storage Capacity (wt%)
AB_5	LaNi ₅	298	1.4
AB_2	$TiMn_2$	298	2.0
AB	TiFe	298	1.86
A_2B	Mg_2Ni	523	3.6

Energies **2025**, 18, 2930 11 of 22

3.3. Temperature and Pressure Conditions of Hydrogen Storage in Alloys

Compared with MOF, the temperature and pressure of alloy hydrogen storage are alleviated, and most alloy materials can achieve stable storage at room temperature and pressure, which greatly reduces the manufacturing cost of hydrogen storage containers [79,80]. It is worth noting that the hydrogen storage process of alloy hydrogen storage materials is carried out at 0.1–1 MPa, 302 K and 333 K, while the hydrogen desorption process requires a significant increase in the temperature of hydrogen storage materials, which brings potential safety risks to the metal hydrogen storage process. The energy consumption of hydrogen storage and desorption process is increased, for example, the hydrogen desorption temperature of LaNi₅ is from 323 to 373 K, the hydrogen desorption temperature of Mg₂Ni is from 523 to 573 K, while the ignition point of hydrogen is about 773 to 844 K, the ignition energy is very low (only 0.02 J), and the combustion range is wide (the volume concentration in air is 4 to 75%) [81]. Therefore, improving the temperature and pressure conditions of alloy hydrogen storage materials is one of the key issues in the development of alloy hydrogen storage technology.

Figure 8 uses visualization methods to systematically present the hydrogen adsorption/desorption characteristic curves of magnesium-based high-entropy alloy composite materials during the programmed temperature control process. The experiment was conducted at a heating rate of 5 K/min, and the experimental scheme is detailed in reference [82]. From Figure 8a, it can be seen that the initial hydrogenation start temperature of the pure magnesium sample (0-MHEA) is 496 K, and the complete hydrogen absorption temperature reaches 676 K. It is worth noting that the introduction of high-entropy alloys significantly reduces the initial hydrogen absorption temperature of MgH2—the initial hydrogen absorption temperatures of 5-MHEA, 10-MHEA and 20-MHEA are, respectively, reduced to 433 K, 427 K and 408 K. Among them, 15-MHEA exhibits the best temperature stability, with the difference between its hydrogenation reaction start temperature (418 K) and termination temperature (595 K) being the smallest, demonstrating excellent kinetic performance.

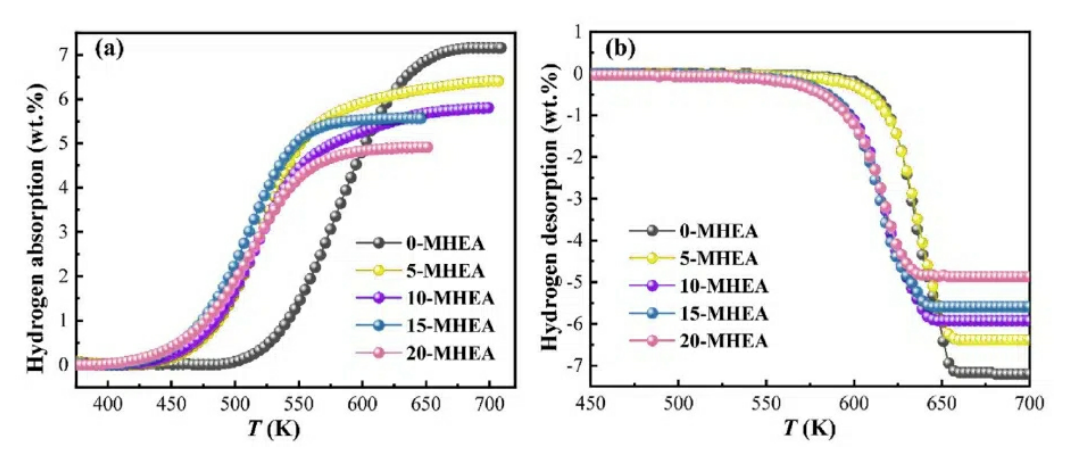


Figure 8. Hydrogen absorption and release curve of Mg-x wt% HEA composite at heating rate of 5 K/min: (a) hydrogen absorption curve, (b) hydrogen emission curve (modified from [82]).

In terms of hydrogen desorption behavior (Figure 8b), 0-MHEA and 5-MHEA exhibited similar desorption characteristics, while 10-MHEA, 15-MHEA and 20-MHEA presented another set of characteristics. Specifically, the initial desorption temperatures of these samples were 573 K (0-MHEA), 558 K (5-MHEA), 531 K (10-MHEA), 526 K (15-MHEA) and 519 K (20-MHEA), respectively. The corresponding desorption completion temperatures showed a regular downward trend. Comprehensive comparison indicates that 15-MHEA demonstrated the best overall performance in both hydrogen absorption and

Energies **2025**, 18, 2930

desorption kinetics and thermodynamics, and exhibited excellent comprehensive hydrogen storage capacity.

3.4. Cyclic Decay of Hydrogen Storage in Alloys

Cyclic decay is one of the key points in the research on hydrogen storage. Usually, the hydrogen storage capacity and rate of materials will decrease to a certain extent after multiple cycles [83]. For example, alloys such as CaNi $_5$ can still maintain a hydrogen storage performance of over 0.96 wt% after 100 cycles [84]. For the La $_{0.65}$ Mg $_{1.32}$ Ca $_{1.03}$ Ni $_9$ alloy, the desorption capacity first increased from 1.43 wt% in the 10th cycle to 1.1 wt% in the 100th cycle, and then gradually decreased, dropping to 0.9 wt% after 300 cycles. Its desorption rate decreased as the number of cycles increased. The change trend of the dehydrogenation rate of the CaNi $_5$ alloy is similar.

Regarding the kinetic decay problem of magnesium-based hydrogen storage materials, the academic community generally adopts catalyst control strategies to enhance their overall performance. Yin et al. [85] innovatively developed a zirconium-based, highly efficient hydrogen storage catalyst. By reconfiguring the Rafes phase structure of magnesium hydrides, they significantly improved the kinetics of hydrogen storage and release. The study showed that the C¹⁵-type intermetallic compound, as a typical highly efficient hydrogen storage phase, not only exhibits outstanding catalytic activity but also enables a fundamental transformation in the rate-limiting step of hydrogen desorption—from the traditional two-dimensional nucleation growth mechanism to a more efficient two-dimensional phase interface migration mode [86,87]. This optimization of the microscopic mechanism directly led to a three-order-of-magnitude improvement in the dehydrogenation kinetics performance of the material (Figure 9).

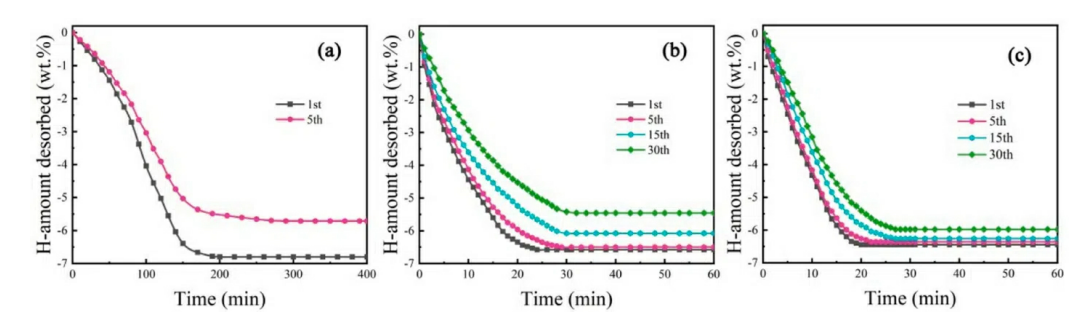


Figure 9. (a) The hydrogen desorption behavior curve of pure MgH_2 under isothermal conditions; (b) the hydrogen absorption/desorption cycle characteristics curve of magnesium-based composite materials with the addition of HEA_1 ; (c) the evolution law of hydrogen cycling performance of the same test conditions in the composite system containing HEA_2 . (modified from [82]).

The results of the cyclic stability test (Figure 9) indicate that after undergoing 30 complete charge–discharge hydrogen cycles, the capacity retention rate of the modified magnesium hydride catalyst remained as high as 92%, fully verifying its outstanding cyclic stability. It is worth noting that the introduction of the C¹⁵ phase structure has produced a dual gain effect: on the one hand, it significantly improves the dehydrogenation efficiency by reducing the hydrogen desorption activation energy; on the other hand, through the unique "hydrogen pump" synergy effect, it optimizes the thermodynamic performance of the entire hydrogen adsorption–desorption process while reducing the operating temperature. The revelation of this multi-cooperative mechanism provides important theoretical support for the development of new high-performance hydrogen storage materials [88].

Energies **2025**, 18, 2930 13 of 22

3.5. Economy of Hydrogen Storage in Alloys

At present, hydrogen storage of alloy materials is one of the few hydrogen storage technologies that have been commercially applied. Table 4 shows Xiamen Tungsten Industry, a Chinese enterprise, that commercializes hydrogen storage of magnesium-based materials [89–91]. From the point of view of operating cost, according to the calculation of hydrogen energy technology, the equipment depreciation and energy consumption of each link in the process are compared from raw gas to the hydrogen filling station. Under the condition of large-scale transportation, when the transport radius is 100 km, the operating cost of magnesium-based solid hydrogen storage is 4 USD/kg [92]. When the transport radius is expanded to 500 km, the operating cost of magnesium-based solid-state hydrogen storage is 20 USD/kg [93–95]. The 2020 DOE report shows that the United States uses NaAlH₄ to achieve hydrogen storage at a cost of 43 USD/kg, while Japan Metals & Chemicals reports LaNi₅ currently studied in Japan costs 15–25 USD/kg, which shows that magnesium-based materials are still one of the cheaper hydrogen storage materials at present.

Table 4. Hydrogen storage cases in various countries.

Country Case	Hydrogen Storage Materials	Cost of Hydrogen Storage
China (Xiamen Tungsten Industry)	Magnesium-based materials	4 USD/kg (within a transport radius of 100 km) 20 USD/kg (within a transport radius of 500 km)
United States (2020 DOE Report)	$NaAlH_4$	43 USD/kg
Japan (Japan Metals & Chemicals)	LaNi ₅	15–25 USD/kg

However, after several cycles of hydrogen absorption and desorption, the alloy material may be pulverized or experience performance attenuation, which will affect its long-term economic use [96]. Although alloy hydrogen storage has the advantages of hydrogen storage density and safety, its high cost and low mass hydrogen storage rate make it an economic challenge in large-scale applications [97,98]. In the future, its economy is expected to be further improved through material optimization, large-scale production and integration with other hydrogen storage technologies.

4. Hydrate Hydrogen Storage

4.1. Concept of Hydrogen Hydrate

Hydrate hydrogen storage is a new hydrogen storage technology with significant advantages; its hydrogen storage density can reach 5.3 wt% [99]. Hydrates are stable at room temperature and pressure, typically with decomposition temperatures of 273–283 K, and are safer and less likely to leak and explode than high-pressure gaseous hydrogen storage (up to 70 MPa) and liquid hydrogen storage (temperatures below 20 K). In addition, hydrate hydrogen storage is environmentally friendly, only water and hydrogen are produced after decomposition, no harmful by-products, and the cost is low; the main raw materials are water and a small amount of accelerator (such as tetrahydrofuran, THF), and its material cost is about 5–10 USD/kg hydrogen, which is much lower than the cost of high-pressure gaseous hydrogen storage container (about 15–20 US USD/kg hydrogen) and the cost of liquid hydrogen storage cryogenic equipment (about 20–30 USD/kg hydrogen). Hydrate hydrogen storage also has the characteristics of rapid hydrogen charging and

Energies **2025**, 18, 2930 14 of 22

discharging, and hydrogen release can be completed within 5–15 min under the condition of 273 K–283 K, which is suitable for application scenarios with frequent hydrogen charging and discharging, such as fuel cell vehicles. At the same time, the hydrate can be stably stored for several days to weeks at room temperature, suitable for long-term storage and transportation, and can operate in the temperature range of 253 K–283 K, with strong adaptability. Although further research and optimization are still needed, hydrate hydrogen storage technology has shown great potential in the field of hydrogen energy storage and transportation, and is expected to become an important hydrogen storage method in the future.

Although hydrate hydrogen storage technology has significant advantages in terms of high hydrogen storage density (up to 5.3 wt%), safety (stable at room temperature and pressure), and environmental protection (only water and hydrogen are produced after decomposition), there are still some key drawbacks that limit its practical application and commercial promotion. Its cycle attenuation is a key challenge, which is mainly manifested in the significant decrease in hydrogen storage capacity, reaction rate and structural stability after multiple hydrogen charging and discharging cycles. Veluswamy et al. [100,101] showed that hydrogen storage capacity may decrease by 20–30% after 10 cycles, e.g., an initial capacity of 5.3 wt% for a tetrahydrofuran (THF) accelerator-based system may be reduced to 3.7–4.2 wt%. At the same time, the structural stability of hydrate hydrogen storage cannot be ignored, and Zhang et al. [102,103] showed that after 50 cycles, the crystal structural integrity of hydrate may decrease by 30-40%, resulting in a decrease in mechanical strength. Temperature has a significant effect on cycle attenuation, and the hydrogen storage capacity may decrease by 40-50% after 10 cycles at 288 K, and only by 20-25% at 273 K. Long-term cycling experiments have shown that after 100 cycles, the hydrogen storage capacity may decrease by 50-60% and the reaction rate may decrease to 30-40% of the initial value [104-106]. These issues need to be addressed through material optimization (e.g., development of novel accelerators), process improvements (e.g., optimization of cycle conditions) and system design (e.g., by-product clean-up mechanisms) to improve the long-term stability and commercialization potential of hydrate hydrogen storage technologies.

4.2. Hydrogen Storage Density of Hydrate

The main factor affecting the theoretical hydrogen storage density of hydrate is the crystal structure. The results show that the crystal structure of hydrate is also different with the addition of a promoter with different properties, which further affects the hydrogen storage density of hydrate [107,108]. It was first found that hydrogen formed sII type hydrate in pure water, and then it was determined that hydrogen would form sI, sH and sC types(semi-cage type) hydrate under specific conditions [109–111].

Kumar et al. [112] synthesized hydrogen hydrate at 140 K and 12 MPa \sim 18 MPa, and discovered that an ice Ic framework has a potentially large H₂ capacity (10 wt% if fully loaded), which has exceeded the theoretical hydrogen storage capacity of sII hydrate.

Papadimitrios et al. [113] simulated and calculated the theoretical hydrogen storage capacity of sI hydrate. The results showed that the hydrogen storage density was 0.37 wt% when the sI-5¹²6² cage held up to three hydrogen molecules and the sI-5¹² cage held one hydrogen molecule at 200 MPa and 270 K. Hydrogen is difficult to exist stably in sI hydrate, and the hydrogen storage capacity is relatively low, so the application prospect of sI hydrate hydrogen storage in hydration hydrogen storage is not great.

Strobel et al. [114] studied the formation of sH-type hydrates with methyl tert-butyl ether (MTBE), methylcyclohexane (MCH), 2,2,3-trimethylbutane (2,2,3-TMB) and 1,1-dimethylcyclohexane (1,1-DMCH) as accelerators. It was found by spectral analysis that

Energies **2025**, *18*, 2930

hydrogen molecules occupied both sH- 5^{12} and sH- $4^35^66^3$ cages, while sH- 5^{12} 6^8 cages were occupied by larger guest molecules. The maximum theoretical hydrogen storage capacity was 1.4 wt%, which was 40% higher than that of sII hydrate (such as THF/H₂ system). In a word, compared with the sII hydrate formed by the H₂/THF system, the hydrogen storage capacity of sH hydrate is higher. However, the higher pressure and lower temperature were required for the synthesis and storage of sH hydrate, which limited its application in hydrogen storage.

The study of Treuba et al. [115] showed that the sC type hydrate formed by 32.33 wt% tetrabutylammonium bromide (TBAB) solution had the maximum hydrogen storage density of 0.046 wt% at 281 K and 16 MPa, and the maximum hydrogen storage density of 0.024 wt% formed by mole fraction 33.82 wt% TBAF (tetrabutylammonium fluoride) hydrate under 13 MPa pressure.

It can be seen from Table 5 and Figure 10 that the hydrogen storage performance of sII hydrate is the best compared with other crystal hydrates. Its hydrogen storage density can be achieved at 5.3 wt%. Although the thermodynamic promoter can improve the forming conditions of hydrogen hydrate, it will reduce the hydrogen storage density. Therefore, finding more efficient promoters or more efficient methods to promote hydrate formation is still the focus of hydrate hydrogen storage research [116,117]. In addition, the different number of hydrogen molecules in the hydrate cage under different conditions also has a great influence on the hydrogen storage of hydrate. The basic research and debate on hydrogen hydrate have been going on [118,119]. It is undeniable that hydrogen hydrate has high energy storage density and is a kind of high energy storage density material with great application prospects.

Table 5. Comparison of temperature and pressure conditions for hydrate formation and hydrogen storage density of several structures.

Crystal Structure	System	Temperature (K)	Pressure (MPa)	Hydrogen Storage Density (wt%)
sI	H_2/CO_2	270	200	0.37
sII	Pure water	273	200~300	5.3
sH	$H_2/MTBE$	270	100	1.4
sc	$H_2/TBAB$	281.15	16	0.046

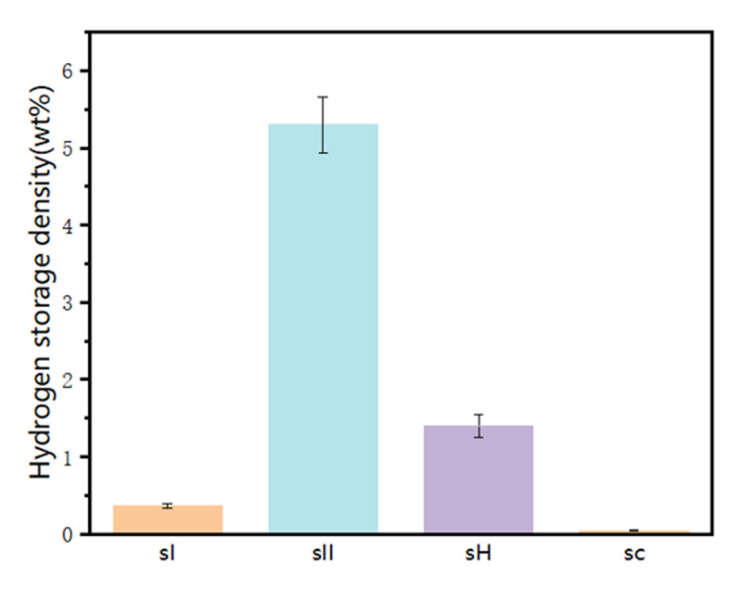


Figure 10. Comparison of hydrogen storage density of hydrate with several structures.

Energies **2025**, 18, 2930 16 of 22

4.3. Temperature and Pressure Conditions for Hydrogen Storage of Hydrate

The existing studies on hydrogen hydrate show that thermodynamic conditions are one of the important conditions for the formation of hydrates. Davoodabadi et al. [120] compared hydrogen hydrate to a hydrogen battery with a fixed structure. Under different stable voltage conditions, the formation and decomposition of hydrogen hydrate is like the charge and discharge of a hydrogen battery, and the coexistence of gas-liquid-solid (hydrate) is the phase equilibrium of the system [121,122]. Figure 11 shows the phase equilibrium interval diagram of several crystal structures of hydrogen hydrate. It can be seen from Figure 11 that for pure water systems, the phase equilibrium conditions of hydrogen hydrate are very harsh. The phase equilibrium pressure is as high as 200 MPa at 260 K, but if it is reduced to 50 MPa, the phase equilibrium temperature is 178 K [123]. Corresponding to this harsh temperature and pressure condition, the phase equilibrium conditions for the formation of hydrogen hydrate have changed significantly after the addition of a hydrate promoter to the system. For example, Hashimoto et al. [124] found that adding 19.04 wt% tetrahydrofuran (THF) to the pure water system could form hydrogen hydrate under the 278 K, 1.55 MPa strip, and adding 40.06 wt% TBAB to the pure water system could form hydrogen hydrate under 286.1 K, 3.27 MPa conditions. Du et al. [125] added 19.26 wt% of tert-butylamine to the pure water system can form hydrogen hydrate under the condition of 273.2 K, 26.12 MPa. Wang et al. [126] injected H_2/C_3H_8 (0.67/0.33) mixture into the pure water system, C₃H₈ acted as a thermodynamic promoter and formed hydrogen hydrate under the condition of 273.72 K, 0.4 MPa.

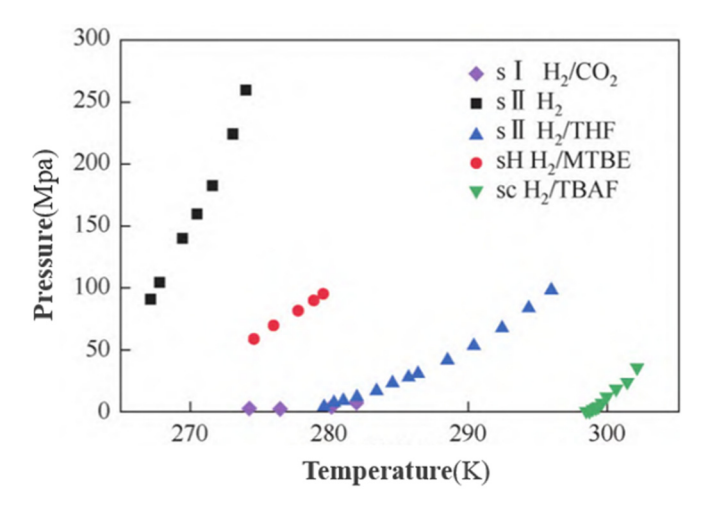


Figure 11. Phase equilibrium diagram of hydrogen hydrate.

4.4. Economy of Hydrogen Storage in Hydrate

Hydrate-based hydrogen storage technology demonstrates significant economic advantages in terms of equipment investment, operational energy consumption and raw material costs. Research shows that the equipment investment cost for hydrate-based hydrogen storage systems can be reduced to USD 5–8 per kilogram H₂, significantly lower than the USD 15–20 per kilogram H₂ for high-pressure gaseous storage and USD 10–12 per kilogram H₂ for liquid hydrogen storage [127]. Additionally, the operational energy consumption of hydrate-based hydrogen storage is only 30–40% of that of liquid hydrogen storage, thanks to its ability to achieve hydrogen storage under mild conditions (2–10 MPa, 253 K to 283 K), avoiding the high-energy-consuming cryogenic cooling systems required for liquid hydrogen storage [128–130]. Furthermore, the raw materials for hydrate-based hydrogen storage (water and gas) are extremely low-cost [131], and there is no need for expensive materials or complex synthesis processes, further reducing overall costs. These

Energies **2025**, 18, 2930 17 of 22

advantages make hydrate-based hydrogen storage highly economical and commercially viable for large-scale applications [132,133].

5. Conclusions

In this paper, the current mainstream solid-state hydrogen storage technologies are reviewed, and the hydrogen storage density, temperature and pressure conditions, cycle decay and economy are compared and analyzed, and the following conclusions are drawn: First, in terms of hydrogen storage density, MOF materials can reach ~5.0 wt%, metal materials can reach 3.6 wt%, and sII hydrate can reach 5.3 wt% under 200~300 MPa conditions. Secondly, through the comparative analysis of the temperature and pressure conditions of hydrogen storage, it can be found that both metal materials and MOF materials can store hydrogen at room temperature and pressure, while hydrate needs to be stored under 200~300 MPa and 273 K, which is also the main bottleneck for hydrate to realize industrial hydrogen storage. Third, from the point of view of cyclic decay, alloys need a large specific surface area and high Gibbs free energy to achieve high cyclic decay. In the process of cyclic hydrogen storage, the original particles will gradually merge into large particles and inhibit hydrogen storage density and rate. Hydrate shows good cyclical stability in the process of cyclic hydrogen storage, and it also has the advantages of low hydrogen storage cost and good hydrogen storage safety. Because of these advantages, hydrate still has a large potential for research and utilization. The development and maturity of hydrate hydrogen storage technology will provide a reliable choice for the arrival of the era of the hydrogen energy economy.

Author Contributions: Conceptualization, D.L. and S.F.; methodology, Z.K.; investigation, G.C.; writing—original draft preparation, G.C.; writing—review and editing, X.Z.; supervision, J.F.; funding acquisition, S.F. All authors have read and agreed to the published version of the manuscript.

Funding: National Natural Science Foundation of China: 51706230.

Data Availability Statement: The data presented in this study are only available on request from the corresponding author due to privacy issues.

Conflicts of Interest: The authors declare no conflicts of interest.

References

- 1. Zou, C.; Ma, F.; Pan, S.; Lin, M.; Zhang, G.; Xiong, B.; Wang, Y.; Liang, Y.; Yang, Z. Earth energy evolution, human development and carbon neutral strategy. *Pet. Explor. Dev.* **2022**, *49*, 468–488. [CrossRef]
- 2. Lee, S.-Y.; Lee, J.-H.; Kim, Y.-H.; Kim, J.-W.; Lee, K.-J.; Park, S.-J. Recent progress using solid-state materials for hydrogen storage: A short review. *Processes* **2022**, *10*, 304. [CrossRef]
- 3. Ait Ousaleh, H.; Mehmood, S.; Baba, Y.F.; Bürger, I.; Linder, M.; Faik, A. An analytical review of recent advancements on solid-state hydrogen storage. *Int. J. Hydrogen Energy* **2024**, *52*, 1182–1193.
- 4. Hui, Y.; Wang, M.; Guo, S.; Akhtar, S.; Bhattacharya, S.; Dai, B.; Yu, J. Comprehensive review of development and applications of hydrogen energy technologies in China for carbon neutrality: Technology advances and challenges. *Energy Convers. Manag.* **2024**, 315, 118776. [CrossRef]
- 5. Abazari, R.; Sanati, S.; Bajaber, M.A.; Javed, M.S.; Junk, P.C.; Nanjundan, A.K.; Qian, J.; Dubal, D.P. Design and Advanced Manufacturing of NU-1000 Metal–Organic Frameworks with Future Perspectives for Environmental and Renewable Energy Applications. *Small* **2024**, *20*, 2306353. [CrossRef] [PubMed]
- 6. Addai, F.P.; Wu, J.; Lin, F.; Ma, X.; Han, J.; Liu, Y.; Zhou, Y.; Wang, Y. Alloyed Trimetallic Nanocomposite as an Efficient and Recyclable Solid Matrix for Ideonella sakaiensis Lipase Immobilization. *Langmuir* **2024**, *40*, 8921–8938. [CrossRef]
- 7. Pleshivtseva, Y.; Derevyanov, M.; Pimenov, A.; Rapoport, A. Comparative analysis of global trends in low carbon hydrogen production towards the decarbonization pathway. *Int. J. Hydrogen Energy* **2023**, *48*, 32191–32240. [CrossRef]
- 8. Chai, H.; Chen, J.; Yu, Y.; Zhao, C. Grand canonical monte carlo simulations of Cu&Li-based metal organic framework for desirable hydrogen storage. *Int. J. Hydrogen Energy* **2024**, *61*, 424–431. [CrossRef]

Energies **2025**, 18, 2930 18 of 22

9. Dai, B.; Shen, X.; Chen, T.; Li, J.; Xu, Q. Porous layered ZnV₂O₄@C synthesized based on a bimetallic MOF as a stable cathode material for aqueous zinc ion batteries. *Dalton Trans.* **2024**, *53*, 8335–8346. [CrossRef]

- 10. Dai, Z.Y.; Zhang, B.; Kimura, H.; Xiao, L.R.; Liu, R.H.; Ni, C.; Hou, C.X.; Sun, X.Q.; Zhang, Y.P.; Yang, X.Y.; et al. Vermiform Ni@CNT derived from one-pot calcination of Ni-MOF precursor for improving hydrogen storage of MgH₂. *Trans. Nonferrous Met. Soc. China* **2024**, *34*, 2629–2644. [CrossRef]
- 11. Granja-DelRío, A.; Cabria, I. Grand Canonical Monte Carlo simulations of the hydrogen and methane storage capacities of JLU-MOF120 and JLU-MOF121. *Int. J. Hydrogen Energy* **2024**, *61*, 57–72. [CrossRef]
- 12. Hu, Q.; Liu, S.; Liu, J.; Lin, M.; Ye, R.; Chen, X. Ultrafast Hole Preservation with Undercoordinated Tungsten for Efficient Solar-to-Chemical Conversion. *ACS Energy Lett.* **2024**, *9*, 3252–3260. [CrossRef]
- 13. Hoang, T.K.; Antonelli, D.M. Exploiting the Kubas interaction in the design of hydrogen storage materials. *Adv. Mater.* **2009**, 21, 1787–1800. [CrossRef]
- 14. Berijani, K.; Vakili-Nezhaad, G.R. The performance of MOFs and rich structure types of stable Zr-MOFs in storing clean energy: Hydrogen. *J. Energy Storage* **2025**, *116*, 115928. [CrossRef]
- 15. Dincă, M.; Long, J.R. Hydrogen storage in microporous metal–organic frameworks with exposed metal sites. *Angew. Chem. Int.* **2008**, 47, 6766–6779. [CrossRef]
- 16. Jing, Y.; Gong, F.; Wang, S.; Wang, W.; Yang, P.; Fu, E.; Xiao, R. Activating the synergistic effect in Ni-Co bimetallic MOF for enhanced plasma-assisted ammonia synthesis. *Fuel* **2024**, *368*, 131686. [CrossRef]
- 17. Al-Roomi, Y.; George, R.; Elgibaly, A.; Elkamel, A. Engineering. Use of a novel surfactant for improving the transportability/transportation of heavy/viscous crude oils. *J. Pet. Sci. Eng.* **2004**, *42*, 235–243. [CrossRef]
- 18. Berry, G.D.; Pasternak, A.D.; Rambach, G.D.; Smith, J.R.; Schock, R.N. Hydrogen as a future transportation fuel. *Energy* **1996**, 21, 289–303. [CrossRef]
- 19. Sakintuna, B.; Lamari-Darkrim, F.; Hirscher, M. Metal hydride materials for solid hydrogen storage: A review. *Int. J. Hydrogen Energy* **2007**, 32, 1121–1140. [CrossRef]
- Irani, R. Hydrogen storage: High-pressure gas containment. MRS Bull. 2002, 27, 680–682. [CrossRef]
- 21. Züttel, A. Hydrogen storage methods. *Naturwissenschaften* **2004**, *91*, 157–172. [CrossRef] [PubMed]
- 22. Rusman, N.; Dahari, M. A review on the current progress of metal hydrides material for solid-state hydrogen storage applications. *Int. J. Hydrogen Energy* **2016**, *41*, 12108–12126. [CrossRef]
- 23. Dornheim, M.; Baetcke, L.; Akiba, E.; Ares, J.-R.; Autrey, T.; Barale, J.; Baricco, M.; Brooks, K.; Chalkiadakis, N.; Charbonnier, V.; et al. Research and development of hydrogen carrier based solutions for hydrogen compression and storage. *Prog. Energy* **2022**, *4*, 042005. [CrossRef]
- 24. Bouwman, P. Applications. In *Fundamentals of Electrochemical Hydrogen Compression*; Bessarabov, D., Wang, H., Li, H., Zhao, N., Eds.; CRC Press: Boca Raton, FL, USA, 2015; pp. 269–299.
- 25. Badwal, S.P.; Giddey, S.S.; Munnings, C.; Bhatt, A.I.; Hollenkamp, A.F. Emerging electrochemical energy conversion and storage technologies. *Front. Chem.* **2014**, *2*, 79. [CrossRef]
- 26. Chung, C.; Ihm, J.; Lee, H. Recent progress on Kubas-type hydrogen-storage nanomaterials: From theories to experiments. *J. Korean Phys. Soc.* **2015**, *66*, 1649–1655. [CrossRef]
- 27. Mahamiya, V.; Dewangan, J.; Chakraborty, B. Interplay between van der Waals, Kubas, and chemisorption process when hydrogen molecules are adsorbed on pristine and Sc-functionalized BeN4. *Int. J. Hydrogen Energy* **2024**, *50*, 1302–1316. [CrossRef]
- 28. Salehabadi, A.; Ahmad, M.I.; Ismail, N.; Morad, N.; Enhessari, M. Solid-state hydrogen storage materials. In *Energy, Society and the Environment*; Springer: Berlin/Heidelberg, Germany, 2020; pp. 41–67. [CrossRef]
- 29. David, E. An overview of advanced materials for hydrogen storage. J. Mater. Process. Technol. 2005, 162-63, 169-177. [CrossRef]
- 30. Dresselhaus, M.S.; Williams, K.A.; Eklund, P.C. Hydrogen Adsorption in Carbon Materials. MRS Bull. 1999, 24, 45–50. [CrossRef]
- 31. Sherif, S.A.; Barbir, F.; Veziroglu, T.N. Towards a Hydrogen Economy. Electr. J. 2005, 18, 62–76. [CrossRef]
- 32. Wan, L.; Zhang, W.; Xu, Z. Overview of Key Technologies and Applications of Hydrogen Energy Storage in Integrated Energy Systems. In Proceedings of the 2020 12th IEEE PES Asia-Pacific Power and Energy Engineering Conference (APPEEC), Nanjing, China, 20–23 September 2020; pp. 1–5.
- 33. Alnafisah, M.S.; Alharbi, K.N.; Almuqati, N.S.; Almalahi, K.M.; Almusawa, M.H.; Almotairy, D.D.; Alotaibi, G.; Alromaeh, A.I. Effect of solvent selection on Zn-MOFs synthesized for hydrogen storage applications. *Int. J. Hydrogen Energy* **2025**, *120*, 393–402. [CrossRef]
- 34. Liu, W.; Yin, R.; Xu, X.; Zhang, L.; Shi, W.; Cao, X. Structural Engineering of Low-Dimensional Metal–Organic Frameworks: Synthesis, Properties, and Applications. *Adv. Sci.* **2019**, *6*, 1802373. [CrossRef] [PubMed]
- 35. Sutton, A.L.; Mardel, J.I.; Hill, M.R. Metal-Organic Frameworks (MOFs) as Hydrogen Storage Materials at Near-Ambient Temperature. *Chem. A Eur. J.* **2024**, *30*, e202400717. [CrossRef] [PubMed]
- 36. Yifu, C. Metal-organic frameworks: Current trends, challenges, and future prospects. Met. Org. Framew. 2024, 3–23.

Energies **2025**, 18, 2930 19 of 22

37. Goel, N. Porous coordination polymers: A brief introduction. In *Porous Coordination Polymers*; Elsevier: Amsterdam, The Netherlands, 2024; pp. 1–9.

- 38. Li, X.; Zhang, G.; Li, N.; Xu, Q.; Li, H.; Lu, J.; Chen, D. Solar-driven production of highly concentrated hydrogen peroxide by Zn3In2S6/PCN-222 heterostructure. *Nano Energy* **2024**, *126*, 109671. [CrossRef]
- 39. Liu, S.; Zhang, Y.; Zhu, F.; Liu, J.; Wan, X.; Liu, R.; Liu, X.; Shang, J.X.; Yu, R.; Feng, Q.; et al. Mg-MOF-74 Derived Defective Framework for Hydrogen Storage at Above-Ambient Temperature Assisted by Pt Catalyst. *Adv. Sci.* 2024, 11, e2401868. [CrossRef]
- 40. Makhafola, M.D.; Balogun, S.A.; Modibane, K.D. A Comprehensive Review of Bimetallic Nanoparticle–Graphene Oxide and Bimetallic Nanoparticle–Metal–Organic Framework Nanocomposites as Photo-, Electro-, and Photoelectrocatalysts for Hydrogen Evolution Reaction. *Energies* 2024, 17, 1646. [CrossRef]
- 41. Rosi, N.L.; Eckert, J.; Eddaoudi, M.; Vodak, D.T.; Kim, J.; O'Keeffe, M.; Yaghi, O.M. Hydrogen storage in microporous metalorganic frameworks. *Science* **2003**, *300*, 1127–1129. [CrossRef]
- 42. Schoedel, A.; Ji, Z.; Yaghi, O.M. The role of metal–organic frameworks in a carbon-neutral energy cycle. *Nat. Energy* **2016**, *1*, 16034. [CrossRef]
- 43. Han, S.S.; Goddard, W.A. Lithium-Doped Metal-Organic Frameworks for Reversible H2 Storage at Ambient Temperature. *J. Am. Chem. Soc.* **2007**, 129, 8422–8423. [CrossRef]
- 44. Chu, C.-L.; Chen, J.-R.; Lee, T.-Y. Enhancement of hydrogen adsorption by alkali-metal cation doping of metal-organic framework-5. *Int. J. Hydrogen Energy* **2012**, *37*, 6721–6726. [CrossRef]
- 45. Xiang, Z.; Hu, Z.; Yang, W.; Cao, D. Lithium doping on metal-organic frameworks for enhancing H2 Storage. *Int. J. Hydrogen Energy* **2012**, *37*, 946–950. [CrossRef]
- Meng, Z.; Lu, R.; Rao, D.; Kan, E.; Xiao, C.; Deng, K. Catenated metal-organic frameworks: Promising hydrogen purification materials and high hydrogen storage medium with further lithium doping. *Int. J. Hydrogen Energy* 2013, 38, 9811–9818. [CrossRef]
- 47. Sengupta, D.; Melix, P.; Bose, S.; Duncan, J.; Wang, X.; Mian, M.R.; Kirlikovali, K.O.; Joodaki, F.; Islamoglu, T.; Yildirim, T.; et al. Air-stable Cu (I) metal-organic framework for hydrogen storage. *J. Am. Chem. Soc.* **2023**, *145*, 20492–20502. [CrossRef] [PubMed]
- 48. Marquez, R.A.; Obeso, J.L.; Vaidyula, R.R.; López-Cervantes, V.B.; Peralta, R.A.; Marín Rosas, P.; de los Reyes, J.A.; Mullins, C.B.; Ibarra, I.A. From pollution to energy storage: Leveraging hydrogen sulfide with SU-101 cathodes in lithium-sulfur batteries. *J. Mater. Chem. A* 2024, 12, 32735–32744. [CrossRef]
- 49. Nguyen, Q.H.; Im, K.; Tu, T.N.; Park, J.; Kim, J. ZIF67-derived ultrafine Co9S8 nanoparticles embedded in nitrogen-doped hollow carbon nanocages for enhanced performances of trifunctional ORR/OER/HER and overall water splitting. *Carbon Lett.* **2024**, *34*, 1915–1925. [CrossRef]
- 50. Jia, T.; Gu, Y.; Li, F. Progress and potential of metal-organic frameworks (MOFs) for gas storage and separation: A review. *J. Environ. Chem. Eng.* **2022**, *10*, 108300. [CrossRef]
- 51. Dewangan, S.K.; Mohan, M.; Kumar, V.; Sharma, A.; Ahn, B. A comprehensive review of the prospects for future hydrogen storage in materials-application and outstanding issues. *Int. J. Energy Res.* **2022**, *46*, 16150–16177. [CrossRef]
- 52. Zhang, K.; Yan, S.; Wu, C.; Park, S.-S.; Ye, J.; Wu, Y. Advancing integrated high–energy metal–gas batteries. *J. Power Sources* **2024**, 612, 234797. [CrossRef]
- 53. Prabu, S.; Vinu, M.; Mariappan, A.; Dharman, R.K.; Oh, T.H.; Chiang, K.Y. Synthesis of Cr(OH)3/ZrO2@Co-based metalorganic framework from waste poly (ethylene terephthalate) for hydrogen production via formic acid dehydrogenation at low temperature. *Ceram. Int.* **2024**, *50*, 24293–24301. [CrossRef]
- 54. Said, M.I.; Dardir, F.M.; Gabr, R.M.; Ahmed, E.A.; Soliman, M.F.; Abukhadra, M.R. CuMOF@Faujasite nanocomposite as a novel catalyst for hydrogen production. *Appl. Organomet. Chem.* **2024**, *38*, e7455. [CrossRef]
- 55. Seyyedattar, M.; Zendehboudi, S.; Ghamartale, A.; Afshar, M. Advancing hydrogen storage predictions in metal-organic frameworks: A comparative study of LightGBM and random forest models with data enhancement. *Int. J. Hydrogen Energy* **2024**, 69, 158–172. [CrossRef]
- 56. Pollet, B.G.; Staffell, I.; Shang, J.L. Current status of hybrid, battery and fuel cell electric vehicles: From electrochemistry to market prospects. *Electrochim. Acta* **2012**, *84*, 235–249. [CrossRef]
- 57. Ahluwalia, R.K.; Peng, J.K.; Hua, T.Q. Sorbent material property requirements for on-board hydrogen storage for automotive fuel cell systems. *Int. J. Hydrogen Energy* **2015**, 40, 6373–6390. [CrossRef]
- 58. Sinha, N.; Pakhira, S. Hydrogen: A Future Chemical Fuel. In *Photoelectrochemical Hydrogen Generation: Theory, Materials Advances, and Challenges*; Kumar, P., Devi, P., Eds.; Springer Nature Singapore: Singapore, 2022; pp. 1–30.
- 59. Singh, M.K.; Krishnan, S.; Singh, K.; Rai, D.K. CNT Interwoven Cu-MOF: A Synergistic Electrochemical Approach for Solid-State Supercapacitor and Hydrogen Evolution Reaction. *Energy Fuels* **2024**, *38*, 12098–12110. [CrossRef]
- 60. Zhang, X.; Zhai, Z.; Feng, X.; Hou, H.; Zhang, Y. Recent Advances of Metal–Organic Framework for Heavy Metal Ions Adsorption. *Langmuir* **2024**, *40*, 17868–17888. [CrossRef]
- 61. Han, L. Engineering Smart Thermal Properties in Metal-Organic-Frameworks. Ph.D. Thesis, University of California, Riverside, CA, USA, 2018.

Energies **2025**, 18, 2930 20 of 22

62. Osman, A.I.; Chen, Z.; Elgarahy, A.M.; Farghali, M.; Mohamed, I.M.A.; Priya, A.K.; Hawash, H.B.; Yap, P.-S. Membrane Technology for Energy Saving: Principles, Techniques, Applications, Challenges, and Prospects. *Adv. Energy Sustain. Res.* **2024**, *5*, 2400011. [CrossRef]

- 63. Liu, F.; Zhang, N. Strategy of Purifier Selection and Integration in Hydrogen Networks. *Chem. Eng. Res. Des.* **2004**, *82*, 1315–1330. [CrossRef]
- 64. Thomas, K.M. Hydrogen adsorption and storage on porous materials. Catal. Today 2007, 120, 389–398. [CrossRef]
- 65. Wang, X.; Breunig, H.M.; Peng, P. Broad range material-to-system screening of metal–organic frameworks for hydrogen storage using machine learning. *Appl. Energy* **2025**, *383*, 125346. [CrossRef]
- 66. Minuto, F.D.; Rozzi, E.; Borchiellini, R.; Lanzini, A. Modeling hydrogen storage at room temperature: Adsorbent materials for boosting pressure reduction in compressed H2 tanks. *J. Energy Storage* **2024**, *90*, 111758. [CrossRef]
- 67. Hamdy, S.; Morosuk, T.; Tsatsaronis, G. Exergetic and economic assessment of integrated cryogenic energy storage systems. *Cryogenics* **2019**, *99*, 39–50. [CrossRef]
- 68. Mayo, S.L.; Olafson, B.D.; Goddard, W.A. DREIDING: A generic force field for molecular simulations. *J. Phys. Chem.* **1990**, 94, 8897–8909. [CrossRef]
- 69. Yang, F.; Wang, J.; Zhang, Y.; Wu, Z.; Zhang, Z.; Zhao, F.; Huot, J.; Grobivć Novaković, J.; Novaković, N. Recent progress on the development of high entropy alloys (HEAs) for solid hydrogen storage: A review. *Int. J. Hydrogen Energy* **2022**, *47*, 11236–11249. [CrossRef]
- 70. Principi, G.; Agresti, F.; Maddalena, A.; Lo Russo, S. The problem of solid state hydrogen storage. *Energy* **2009**, *34*, 2087–2091. [CrossRef]
- 71. Yeh, J.W.; Chen, S.K.; Lin, S.J.; Gan, J.Y.; Chin, T.S.; Shun, T.T.; Tsau, C.H.; Chang, S.Y. Nanostructured high-entropy alloys with multiple principal elements: Novel alloy design concepts and outcomes. *Adv. Eng. Mater.* **2004**, *6*, 299–303. [CrossRef]
- 72. Cantor, B.; Chang, I.T.; Knight, P.; Vincent, A.J. Microstructural development in equiatomic multicomponent alloys. *Mater. Sci. Eng. A* **2004**, 375, 213–218. [CrossRef]
- 73. Sandrock, G. A panoramic overview of hydrogen storage alloys from a gas reaction point of view. *J. Alloys Compd.* **1999**, 293, 877–888. [CrossRef]
- 74. Panwar, K.; Srivastava, S. Theoretical model on the electronic properties of multi-element AB5-type metal hydride. *Int. J. Hydrogen Energy* **2021**, *46*, 10819–10829. [CrossRef]
- 75. Xie, D. Effect of Surface Coating on Electrochemical Properties of Rare Earth-Based AB5-type Hydrogen Storage Alloys. *Int. J. Electrochem. Sci.* **2016**, *11*, 9153–9163. [CrossRef]
- 76. Young, K.; Chao, B.; Liu, Y.; Nei, J. Microstructures of the oxides on the activated AB2 and AB5 metal hydride alloys surface. *J. Alloys Compd.* **2014**, *606*, 97–104. [CrossRef]
- 77. Yu, X.; Wu, Z.; Xia, B.; Huang, T.; Chen, J.; Wang, Z.; Xu, N. Hydrogen storage in Ti–V-based body-centered-cubic phase alloys. *J. Mater. Res.* **2003**, *18*, 2533–2536. [CrossRef]
- 78. Yang, B.; He, J.; Zhang, G.; Guo, J. Vanadium Series Products and Functional Materials. *Vanadium Extr. Manuf. Appl.* **2021**, 395–413.
- 79. Shet, S.P.; Shanmuga Priya, S.; Sudhakar, K.; Tahir, M. A review on current trends in potential use of metal-organic framework for hydrogen storage. *Int. J. Hydrogen Energy* **2021**, *46*, 11782–11803. [CrossRef]
- 80. Luo, Y.; Wang, Q.; Li, J.; Xu, F.; Sun, L.; Zou, Y.; Chu, H.; Li, B.; Zhang, K. Enhanced hydrogen storage/sensing of metal hydrides by nanomodification. *Mater. Today Nano* **2020**, *9*, 100071. [CrossRef]
- 81. Yang, X.; Lu, X.; Zhang, J.; Hou, Q.; Zou, J. Progress in improving hydrogen storage properties of Mg-based materials. *Mater. Today Adv.* **2023**, *19*, 100387. [CrossRef]
- 82. Wu, S.; Chen, Y.; Kang, W.; Cai, X.; Zhou, L. Hydrogen storage properties of MgTiVZrNb high-entropy alloy and its catalytic effect upon hydrogen storage in Mg. *Int. J. Hydrogen Energy* **2024**, *50*, 1113–1128. [CrossRef]
- 83. Sadhasivam, T.; Kim, H.-T.; Jung, S.; Roh, S.-H.; Park, J.-H.; Jung, H.-Y. Dimensional effects of nanostructured Mg/MgH2 for hydrogen storage applications: A review. *Renew. Sustain. Energy Rev.* **2017**, 72, 523–534. [CrossRef]
- 84. Ding, X.; Chen, R.; Chen, X.; Cao, W.; Su, Y.; Ding, H.; Guo, J. Formation of Mg2Ni/Cu phase and de-/hydrogenation behavior of Mg91Ni9-xCux alloy at moderate temperatures. *Renew. Energy* **2020**, *166*, 81–90. [CrossRef]
- 85. Yin, F.; Chen, Z.; Si, T.; Liu, D.; Li, Y.; Li, H.-W.; Zhang, Q. Structural-regulation of Laves phase high-entropy alloys to catalytically enhance hydrogen desorption from MgH2. *J. Alloys Compd.* **2024**, *997*, 174822. [CrossRef]
- 86. Van Vleet, M.J.; Weng, T.; Li, X.; Schmidt, J.R. In Situ, Time-Resolved, and Mechanistic Studies of Metal–Organic Framework Nucleation and Growth. *Chem. Rev.* **2018**, *118*, 3681–3721. [CrossRef]
- 87. Dansirima, P.; Pangon, A.; Utke, O.; Utke, R. Dehydrogenation kinetics of MgH2-based hydrogen storage tank at different operating temperatures and mass flow rates. *Int. J. Hydrogen Energy* **2022**, *47*, 7351–7361. [CrossRef]
- 88. Wan, H.; Yang, X.; Zhou, S.; Ran, L.; Lu, Y.; Chen, Y.; Wang, J.; Pan, F. Enhancing hydrogen storage properties of MgH2 using FeCoNiCrMn high entropy alloy catalysts. *J. Mater. Sci. Technol.* **2023**, *149*, 88–98. [CrossRef]

Energies **2025**, *18*, 2930 21 of 22

89. Yadav, Y.K.; Shaz, M.A.; Yadav, T.P. Al–Cu–Fe–Ni–Ti high entropy alloy nanoparticles as new catalyst for hydrogen sorption in MgH2. *Int. J. Hydrogen Energy* **2024**. [CrossRef]

- 90. Zhang, X.L.; Liu, Y.F.; Zhang, X.; Hu, J.J.; Gao, M.X.; Pan, H.G. Empowering hydrogen storage performance of MgH2 by nanoengineering and nanocatalysis. *Mater. Today Nano* **2020**, *9*, 100064. [CrossRef]
- 91. Yu, R.; Yang, C.; Liu, R.; Xu, Z.; Hu, C.; Xia, L.; Jin, Y.; Liu, X.; Shui, J. Tungsten clusters derived from phosphotungstic acid to enhance hydrogen storage efficiency in MgH2. *Int. J. Hydrogen Energy* **2024**, *55*, 778–785. [CrossRef]
- 92. Zhang, G.; Jiang, Z. Overview of hydrogen storage and transportation technology in China. *Unconv. Resour.* **2023**, *3*, 291–296. [CrossRef]
- 93. Zhou, Y.; Luo, L.; Yan, W.; Li, Z.; Fan, M.; Du, G.; Zhao, W. Controlled preparation of nitrogen-doped hierarchical carbon cryogels derived from Phenolic-Based resin and their CO2 adsorption properties. *Energy* **2022**, *246*, 123367. [CrossRef]
- 94. Ghorbani, B.; Zendehboudi, S.; Saady, N.M.C.; Dusseault, M.B. Hydrogen storage in North America: Status, prospects, and challenges. *J. Environ. Chem. Eng.* **2023**, *11*, 109957. [CrossRef]
- 95. Liu, H.; Zhang, J.; Sun, P.; Zhou, C.; Liu, Y.; Fang, Z.Z. An overview of TiFe alloys for hydrogen storage: Structure, processes, properties, and applications. *J. Energy Storage* **2023**, *68*, 107772. [CrossRef]
- 96. Chen, Y.; Zhao, S.; Ma, H.; Wang, H.; Hua, L.; Fu, S. Analysis of Hydrogen Embrittlement on Aluminum Alloys for Vehicle-Mounted Hydrogen Storage Tanks: A Review. *Metals* **2021**, *11*, 1303. [CrossRef]
- 97. Xu, Y.; Zhou, Y.; Li, Y.; Hao, Y.; Wu, P.; Ding, Z. Magnesium-Based Hydrogen Storage Alloys: Advances, Strategies, and Future Outlook for Clean Energy Applications. *Molecules* **2024**, *29*, 2525. [CrossRef] [PubMed]
- 98. Kojima, Y. Hydrogen storage materials for hydrogen and energy carriers. Int. J. Hydrogen Energy 2019, 44, 18179–18192. [CrossRef]
- 99. Mao, W.L.; Mao, H.-K. Hydrogen storage in molecular compounds. Proc. Natl. Acad. Sci. USA 2004, 101, 708-710. [CrossRef]
- 100. Cai, X.; Worley, J.; Phan, A.; Salvalaglio, M.; Koh, C.; Striolo, A. Understanding the effect of moderate concentration SDS on CO2 hydrates growth in the presence of THF. *J. Colloid Interface Sci.* **2024**, *658*, 1–11. [CrossRef]
- 101. Fiedler, F.; Vinš, V.; Jäger, A.; Span, R. Modification of the van der Waals and Platteeuw model for gas hydrates considering multiple cage occupancy. *J. Chem. Phys.* **2024**, *160*. [CrossRef] [PubMed]
- 102. Han, G.; Lee, W.; Kim, M.K.; Lee, J.W.; Ahn, Y.H. Hydrogen separation from hydrogen-compressed natural gas blends through successive hydrate formations. *Chem. Eng. J.* **2024**, *483*, 149409. [CrossRef]
- 103. Hu, W.; Tian, X.; Chen, C.; Cheng, C.; Zhu, S.; Zhang, J.; Qi, T.; Jin, T.; Wu, X. Molecular dynamic simulation of H2-CH4 binary hydrate growth induced by methane hydrate. *Fuel* **2024**, *360*, 130554. [CrossRef]
- 104. Suzuki, K.; Wada, R.; Konno, Y.; Hiekata, K.; Nanjo, T.; Nagakubo, S. Impact of epistemic uncertainty on tradeoff in model-based decision support for methane hydrate development system design. *Appl. Energy* **2024**, *356*, 122408. [CrossRef]
- 105. Wang, P.; Long, H.; Teng, Y.; Li, Y.; Li, Y.; Zhu, J.; Xie, H.; Han, S.; Zhao, Y.; Zhu, J. Investigation of hydrogen-propane hydrate formation mechanism and optimal pressure range via hydrate-based hydrogen storage. *Fuel* **2024**, *361*, 130791. [CrossRef]
- 106. Xu, H.; Liu, Y.; He, S.; Zheng, J.N.; Jiang, L.; Song, Y. Enhanced CO2 hydrate formation using hydrogen-rich stones, L-Methionine and SDS: Insights from kinetic and morphological studies. *Energy* **2024**, 291, 130280. [CrossRef]
- 107. Khan, M.N. Hydrogen as future sustainable energy resource: An insight into technological advancements in hydrate-based hydrogen storage. *Int. J. Hydrogen Energy* **2025**, *97*, 1386–1398. [CrossRef]
- 108. Kim, M.K.; Ahn, Y.H. Gas Hydrates for Hydrogen Storage: A Comprehensive Review and Future Prospects. *Korean J. Chem. Eng.* **2024**, *41*, 73–94. [CrossRef]
- 109. Krishna, S.; Mahant, B.; Robustillo, M.D.; Sreenivasan, H.; Pandey, J.S. The Role of Gas Hydrates in Storing Natural Gas-Hydrogen Blends for Coupling Power-to-X and Decarbonization. *Energy Fuels* **2024**, *38*, 23192–23229. [CrossRef]
- 110. Kummamuru, N.B.; Ciocarlan, R.G.; Houlleberghs, M.; Martens, J.; Breynaert, E.; Verbruggen, S.W.; Cool, P.; Perreault, P. Surface modification of mesostructured cellular foam to enhance hydrogen storage in binary THF/H2 clathrate hydrate. *Sustain. Energy Fuels* 2024, *8*, 2824–2838. [CrossRef]
- 111. Lan, X.; Chen, J.; Li, D.; Zheng, J.; Linga, P. Gas storage via clathrate hydrates: Advances, challenges, and prospects. *Gas Sci. Eng.* **2024**, *129*, 205388. [CrossRef]
- 112. Kumar, R.; Klug, D.D.; Ratcliffe, C.I.; Tulk, C.A.; Ripmeester, J.A. Low-pressure synthesis and characterization of hydrogen-filled ice Ic. *ChemInform* **2013**, *125*, 1571.
- 113. Papadimitriou, N.I.; Tsimpanogiannis, I.N.; Papaioannou, A.T.; Stubos, A.K. Evaluation of the Hydrogen-Storage Capacity of Pure H2 and Binary H2-THF Hydrates with Monte Carlo Simulations. *J. Phys. Chem. C* **2008**, *112*, 10294–10302. [CrossRef]
- 114. Strobel, T.A.; Koh, C.A.; Sloan, E.D. Water Cavities of sH Clathrate Hydrate Stabilized by Molecular Hydrogen. *J. Phys. Chem. B* **2008**, *112*, 1885–1887. [CrossRef]
- 115. Trueba, A.T.; Radović, I.R.; Zevenbergen, J.F.; Kroon, M.C.; Peters, C.J. Kinetics measurements and in situ Raman spectroscopy of formation of hydrogen–tetrabutylammonium bromide semi-hydrates. *Int. J. Hydrogen Energy* **2012**, *37*, 5790–5797. [CrossRef]
- 116. Lee, W.; Kim, K.; Lee, J.; Ahn, Y.H.; Lee, J.W. Perspectives on facilitating natural gas and hydrogen storage in clathrate hydrates under a static system. *Green Chem.* **2024**, *26*, 7552–7578. [CrossRef]

Energies **2025**, 18, 2930 22 of 22

117. Lin, H.; Wang, Y.; Lang, X.; Li, G.; Lu, E.; Tian, W.; Fan, S. Hydrate-Based Hydrogen Storage and Transportation System: Energy, Exergy, Economic Analysis. In *Lecture Notes in Civil Engineering*; Springer: Singapore, 2024; pp. 405–421.

- 118. Mahant, B.; Kushwaha, O.S.; Kumar, R. Thermodynamic phase equilibria study of Hythane (methane + hydrogen) gas hydrates for enhanced energy storage applications. *Fluid Phase Equilibria* **2024**, *582*, 114089. [CrossRef]
- 119. Mahant, B.; Swethika, C.S.; Kushwaha, O.S.; Kumar, R. Storage and Transportation of Hythane: Thermodynamics, Kinetics, and Stability Studies Using the Gas Hydrates Process. *Energy Fuels* **2024**, *38*, 17586–17607. [CrossRef]
- 120. Davoodabadi, A.; Mahmoudi, A.; Ghasemi, H.J.I. The potential of hydrogen hydrate as a future hydrogen storage medium. *iScience* **2021**, 24, 101907. [CrossRef] [PubMed]
- 121. Majid, A.A. Gas hydrate technological applications: From energy recovery to carbon capture and storage. *Gas Sci. Eng.* **2024**, *131*, 205455. [CrossRef]
- 122. Nguyen, N.N. Prospect and Challenges of Hydrate-Based Hydrogen Storage in the Low-Carbon Future. *Energy Fuels* **2023**, *37*, 9771–9789. [CrossRef]
- 123. Dohrn, R.; Peper, S.; Fonseca, J.M.S. High-pressure fluid-phase equilibria: Experimental methods and systems investigated (2000–2004). *Fluid Phase Equilibria* **2010**, *288*, 1–54. [CrossRef]
- 124. Hashimoto, S.; Murayama, S.; Sugahara, T.; Sato, H.; Ohgaki, K. Thermodynamic and Raman spectroscopic studies on H2+ tetrahydrofuran+ water and H2+ tetra-n-butyl ammonium bromide+ water mixtures containing gas hydrates. *Chem. Eng. Sci.* **2006**, *61*, 7884–7888. [CrossRef]
- 125. Du, J.-W.; Liang, D.-Q.; Dai, X.-X.; Li, D.-L.; Li, X.-J. Hydrate phase equilibrium for the (hydrogen+ tert-butylamine+ water) system. *J. Chem. Thermodyn.* **2011**, 43, 617–621. [CrossRef]
- 126. Wang, P.; Li, K.; Yang, J.; Zhu, J.; Zhao, Y.; Teng, Y. Experimental and theoretical study on dissociation thermodynamics and kinetics of hydrogen-propane hydrate. *Chem. Eng. J.* **2021**, 426, 131279. [CrossRef]
- 127. Zhang, M.; Ni, D. Evaluating the gas storage capacity of 1,3-dioxolane–hydrogen binary hydrates via molecular simulations. *J. Mol. Liq.* **2024**, 393, 123542. [CrossRef]
- 128. Bhattacharjee, G.; Veluswamy, H.P.; Kumar, A.; Linga, P. Stability analysis of methane hydrates for gas storage application. *Chem. Eng. J.* **2021**, *415*, 123542. [CrossRef]
- 129. Borah, U.B.; Pandey, G.; Sarma, S.; Molokitina, N.; Chauhan, G. Affordable and Clean Energy: Natural Gas Hydrates and Hydrogen Storage. In *Clean and Renewable Energy Production*; Wiley-Scrivener: Hoboken, NJ, USA, 2024; pp. 87–121.
- 130. Kong, Y.; Yu, H.; Liu, M.; Zhang, G.; Wang, F. Ultra-rapid formation of mixed H2/DIOX/THF hydrate under low driving force: Important insight for hydrate-based hydrogen storage. *Appl. Energy* **2024**, *362*, 123029. [CrossRef]
- 131. Zhou, S.; Yang, Q.; Liu, Y.; Cheng, L.; Taylor Isimjan, T.; Tian, J.; Yang, X. Electronic metal-support interactions for defect-induced Ru/Co-Sm2O3 mesosphere to achieve efficient NaBH4 hydrolysis activity. *J. Catal.* **2024**, 433, 115491. [CrossRef]
- 132. Zhang, Y.; Bhattacharjee, G.; Kumar, R.; Linga, P. Solidified Hydrogen Storage (Solid-HyStore) via Clathrate Hydrates. *Chem. Eng. J.* 2022, 431, 133702. [CrossRef]
- 133. Zhang, Y.; Bhattacharjee, G.; Linga, P. Kinetic Study of Mixed Hydrogen/1,3-Dioxolane Hydrates in the Presence of Amino Acids. *Energy Proc.* **2021**, *18*, 169.

Disclaimer/Publisher's Note: The statements, opinions and data contained in all publications are solely those of the individual author(s) and contributor(s) and not of MDPI and/or the editor(s). MDPI and/or the editor(s) disclaim responsibility for any injury to people or property resulting from any ideas, methods, instructions or products referred to in the content.